0026-895X/07/7204-984–992$20.00
MOLECULAR PHARMACOLOGY
Vol. 72, No. 4
38018/3252696
Mol Pharmacol 72:984–992, 2007
Printed in U.S.A.

Antithrombotic Effect of a Protein-Type I Class Snake Venom Metalloproteinase, Kistomin, Is Mediated by Affecting Glycoprotein Ib-von Willebrand Factor Interaction

Chun-Chieh Hsu, Wen-Bin Wu, Ya-Hui Chang, Heng-Lan Kuo, and Tur-Fu Huang

Department of Pharmacology, College of Medicine, National Taiwan University, Taipei, Taiwan (C.-C.H., Y.-H.C., H.-L.K., T.-F.H); and School of Medicine, Fu-Jen Catholic University, Taipei County, Taiwan (W.-B.W.)

Received May 10, 2007; accepted July 3, 2007

ABSTRACT

Binding of von Willebrand factor (vWF) to platelet glycoprotein (GP) Ib-IX-V mediates platelet activation in the early stage of thrombus formation. Kistomin, a snake venom metalloproteinase (SVMP) purified from venom of *Calloselasma rhodostoma*, has been shown to inhibit vWF-induced platelet aggregation. However, its action mechanism, structure-function relationship, and in vivo antithrombotic effects are still largely unknown. In the present study, cDNA encoding kistomin precursor was cloned and revealed that kistomin is a P-I class SVMP with only a proteinase domain. Further analysis indicated that kistomin specifically inhibited vWF-induced platelet aggregation through binding and cleavage of platelet GPIbα and vWF. Cleavage of platelet GPIbα by kistomin resulted in release of 45- and 130-kDa soluble fragments, indicating that kistomin cleaves GPIbα at two distinct sites. In parallel, cleavage of vWF by kistomin also resulted in the formation of low-molecular-mass multimers of vWF. In ex vivo and in vivo studies, kistomin cleaved platelet GPIbα in whole blood. Moreover, GPIbα agonist-induced platelet aggregation ex vivo was inhibited, and tail-bleeding time was prolonged in mice administered kistomin intravenously. Kistomin's in vivo antithrombotic effect was also evidenced by prolonging the occlusion time in mesenteric microvessels of mice. In conclusion, kistomin, a P-I class metalloproteinase, has a relative specificity for GPIbα and vWF and its proteolytic activity on GPIbα-vWF is responsible for its antithrombotic activity both in vitro and in vivo. Kistomin can be useful as a tool for studying metalloproteinase-substrate interactions and has a potential being developed as an antithrombotic agent.

Platelets play a key role in hemostasis and thrombosis. Exposure of subendothelial von Willebrand factor (vWF) is the first step to form thrombi to arrest blood loss at the sites of trauma, but abnormal embolism may also cause ischemia in pathogenic condition (Andrews and Berndt, 2004). The glycoprotein (GP) Ib complex (one of the major adhesive receptors expressed on platelets) that interacts with vWF is composed of GPIbα, GPIbβ, GPIX, and GPV. GPIbα consists of N-terminal flank, leucine-rich repeat, anionic sulfated tyrosine sequence, macroglycopeptide domain, transmembrane region, and cytoplasmic tail (Andrews et al., 2003). Plasma vWF circulates primarily as the dimer form, and the multimeric forms of vWF are existed in the subendothelial matrix (Canobbio et al., 2004). It has been reported that Bernard-Soulier syndrome and platelet-type von Willebrand disease are inherited bleeding disorders caused by mutations in *GPIb complex* and *vWF* gene, respectively, suggesting that GPIb-vWF interaction is very important for hemostasis. Therefore, modulation of the GPIbα-vWF interactions during thrombotic complications could be beneficial (Bonnefoy et al., 2003). However, in contrast to extensive application of αIIbβ3 antagonists during acute coronary diseases, no GPIbα-vWF axis inhibitor is commercially available, although some GPIbα or vWF antagonists are being developed.

Snake venom proteases are invaluable tools for studying coagulation and hemostasis (Marsh, 2001). For examples, fibrinogen and antithrombin III can be assayed by using snake venom thrombin-like enzymes. Among these snake-derived proteases, snake venom metalloproteinases (SVMPs), which are abundant in venoms from Viperidae and Crotalinae, are key enzymes responsible for local hemorrhage and are metal ion-dependent for their full function (Matsui et al., 2000; Kamiguti, 2005). The protein structural classification of SVMPs is presented as protein-type I (P-I;

This work was financially supported by National Science Council grant NSC95-2320-B002-045, Taiwan.
Article, publication date, and citation information can be found at http://molpharm.aspetjournals.org.
doi:10.1124/mol.107.038018.

ABBREVIATIONS: vWF, von Willebrand factor; GP, glycoprotein; SVMP, snake venom metalloproteinase; mAb, monoclonal antibody; FITC, fluorescein isothiocyanate; PVDF, polyvinylidene difluoride; PCR, polymerase chain reaction; PRP, platelet-rich plasma; PS, platelet suspension; RT, room temperature; PBS, phosphate-buffered saline; P-I–IV, protein-types I–IV.

having only metalloproteinase domain), P-II (having metalloproteinase and disintegrin domain), P-III (having metalloproteinase, disintegrin-like and cysteine-rich domain), and P-IV (having P-III structure plus lectin-like domains connected by disulfide bonds) (Fox and Serrano, 2005). It has been suggested that the additional disintegrin-like and the cysteine-rich regions domains may direct SVMP to its targets (Fox and Serrano, 2005). However, its structure-activity relationship remains unclear.

Kistomin, a 25-kDa SVMP purified from *Calloselasma rhodostoma* venom in our laboratory, has been shown to degrade fibrinogen and inhibit ristocetin-induced platelet agglutination, suggesting that it is a GPIb-cleaving protease (Huang et al., 1993). However, its action mechanism, structure-function relationship, and in vivo antithrombotic effects are still largely unknown. In this study, cDNA-encoding kistomin was cloned and kistomin's cleaving and binding specificities for vWF and GP Ibα were demonstrated. More importantly, kistomin's antithromblotic effect was examined in an in vivo animal model.

Materials and Methods

Materials. Anti-GPIbα mAb M45 and SZ2, directed to the sulfated tyrosine residues of GPIbα and inhibited ristocetin-dependent binding of vWF to GPIbα, were obtained from CLB Immunoreagentia (Amsterdam, The Netherlands) and Immunotech (Marseilles, France), respectively. The murine mAb against $\alpha 2\beta 1$, 6F1, was kindly provided by Dr. Barry S. Coller (Mount Sinai School of Medicine, New York, NY). FITC-conjugated goat anti-mouse IgG was from Santa Cruz Biotechnology, Inc. (Santa Cruz, CA). Heparin was from Thermo Fisher Scientific (Waltham, MA). Human purified vWF and fibrinogen were from Calbiochem (San Diego, CA). Enhanced chemiluminescence (ECL) Western blotting system was from PerkinElmer Life and Analytical Sciences (Waltham, MA). Other chemicals were purchased from Sigma Chemicals, Co. (St Louis, Mo).

Venoms of *C. rhodostoma, Crotalus atrox,* and *Trimeresurus flavoviridis* were from Latoxan (Rosans, France). Kistomin was purified from crude venom of *C. rhodostoma* as described previously (Huang et al., 1993), migrating as a single band at 25 kDa on SDS-polyacrylamide gel electrophoresis assay. Crotalin (Wu et al., 2001b) and triflamp (Tseng et al., 2004a) were purified from *C. atrox* and *T. flavoviridis*, respectively.

Protein Sequencing of the Fragmented Kistomin and cDNA Cloning of Kistomin Precursor. Protein sequencing of the fragmented kistomin was performed as described previously (Wu et al., 2001a). In brief, fragmented kistomin was obtained by alkylation with vinylpyridine and followed by incubation with CNBr. The fragments were applied to high-performance liquid chromatography, and the major fraction was subjected to protein sequencing. For sequencing of the autoproteolytic fragment of kistomin, kistomin was autoproteolyted in 1% SDS and 0.5 M Tris-HCl solution, transblotted onto PVDF membrane, and then analyzed by sequencing.

Total RNA was isolated from *C. rhodostoma* venom glands with a BlueExtract kit (LTK BioLaboratories Co., Ltd, Linko, Taipei, Taiwan). cDNA was synthesized from 1.5 mg of the total RNA and used to construct a cDNA library in the Uni-ZAP XR vector (Stratagene, La Jolla, CA).

To obtain cDNA of putative SVMP, recombinant λ DNA species were prepared from the cDNA library and used as templates in PCR. Primers for the first screening of cDNA library were 5′-TCCATCGAAGTC(G/A)TTGTT(G/A)AA-3′ and 5′-TCAGGTTGG(C/T)TTGAAAGCAGG-3′. Amplification was performed by using *Taq* DNA polymerse (Ab Peptides, St. Louis, MO) and the primers with a hot start at 94°C for 10 min and 30 cycles of denaturation (1 min, at 94°C), annealing (1 min, at 50°C), and extension (2 min, at 72°C). Primers for the second amplification of the 3′-end of the precursor cDNA of kistomin were 5′-GCGGATAAAAGCATGGTTGA-3′ and M13 forward primer. PCR was performed under the same conditions, except that the primer-annealing temperature was set at 45°C. The final PCR products were analyzed by 1% (w/v) agarose-gel electrophoresis and purified by electroelution. The purified DNA fragments were ligated to pcRII-TOPO vector with a *Thermus aquaticus* cloning kit (Invitrogen, Carlsbad, CA), and sequence analysis was performed. The specificity of the second amplification was confirmed from the overlapping sequences that were distinguishable from the other SVMPs. Sequences were assembled with the GCG program (Wisconsin Package version 10.1; Genetics Computer Group).

Platelet Aggregation. Blood was collected from healthy human volunteers and anticoagulated with 3.8% sodium citrate [9:1 (v/v)]. Citrated blood was immediately centrifuged for 10 min at 120*g* and 25°C, and the supernatant [platelet-rich plasma (PRP)] was obtained. Human washed platelet suspension (PS) was prepared as described previously (Liu et al., 1996) and adjusted to approximately 3.8×10^8 platelets/ml. Platelet aggregation was monitored by light transmission in a Lumi-Aggregometer (Chrono-Log, Havertown, PA) with continuous stirring at 900 rpm at 37°C as described previously (Liu et al., 1996).

For ex vivo assay of mouse platelet aggregation, male ICR mice (12–15 g) were intravenously injected with different dosage of kistomin. After 20 min, mouse was anesthetized with sodium pentobarbital (50 μg/g, ip), and blood was collected by cardiac puncture. PRP was obtained by centrifugation at 200*g* for 4 min at room temperature. After washing twice with Tyrode's solution, platelet suspension was adjusted to approximately 5×10^8 platelets/ml, and aggregation was measured turbidimetrically.

Flow Cytometric Analysis of Platelet Receptor Expression. Washed human platelets were prepared as described above. PS (3.8×10^8 platelets/ml) containing 2 μM PGE_1 was incubated with kistomin 20 μg/ml at 37°C for 10 min. After an extensive wash, platelets were labeled with mAb against GPIbα (SZ2), αIIbβ3 (7E3), or $\alpha 2\beta 1$ integrin (6F1) at room temperature (RT) for 30 min. Labeled cells were washed with Tyrode's solution and then incubated with secondary FITC-conjugated goat antimouse IgG (CALTAG Lab, Burlingame, CA) RT for 30 min with a continuous shaking. After incubation, cells were washed, resuspended in phosphate-buffered saline (PBS), and analyzed immediately by FACSCalibur (BD Biosciences, San Jose, CA).

Western Blot Analysis of Platelet GPIbα. Platelet suspension was centrifuged at 200*g* for 5 min. After removing the supernatant, pellets were lysed by 1% Triton X-100 buffer (in PBS). Aliquots of cell lysates and supernatants were resolved on 10% SDS-PAGE under reducing conditions and electrotransferred to Immobilon-PVDF membrane (Millipore). After blocking in a 0.5% BSA in Tri-buffered saline 1 h at 4°C, the blots were probed with anti-GPIbα mAb (1:1000) for overnight at 4°C and followed by the horseradish peroxidase-goat anti-mouse IgG. The protein was visualized by adding enhanced chemiluminescence (ECL) solution (Pierce, Rockford, IL).

Determination of Kistomin Binding to Platelet GPIbα. For determination of the interaction between kistomin and GPIbα, flow cytometric and Western blot analysis were performed. For flow cytometry, platelets were incubated with or without kistomin at 4°C and followed by probing with FITC-conjugated anti-GPIbα mAb, M45. Cells were analyzed immediately by FACS Calibur (BD Biosciences). For Western blot analysis, kistomin (20 μg) and agglucetin (15 μg) were applied to 15% SDS-PAGE and transferred onto a PVDF membrane. Platelets lysate was obtained by lysis of platelet pellet in lysis buffer (10 mM HEPES buffer containing 10% SDS, 10 mM *N*-ethylmaleimide, 20 mM Na_3VO_4, 20 mM EDTA, and 10 mM phenylmethylsulfonyl fluoride). The membrane was blocked with 1% bovine serum albumin and then incubated with platelet lysate for 1 h at RT. After a brief wash, the membrane was probed with anti-GPIbα SZ2 mAb and developed by ECL.

Cleavage of vWF by Kistomin. Purified human vWF (1.5 μg) incubated with or without kistomin were analyzed as described previously (Wu et al., 2001b) with a minor modification. In brief, aliquots of the mixture were analyzed by SDS-1% agarose gel electrophoresis (~2 mm) in a Mupid-2 Mini-Gel system (Cosmo Bio Co., Ltd, Tokyo, Japan) and electroblotted onto PVDF membrane. Immunoblots were developed with peroxidase-conjugated antihuman vWF antibody (DAKOpatts, Glostrup, Denmark).

Fluorescent Dye-induced Platelet Thrombus Formation in Mesenteric Microvessels of Mice. Fluorescent dye-induced platelet thrombus formation in mesenteric microvessels of mice was performed as described previously (Chang and Huang, 1994) with some modifications. In brief, after male ICR mice (12–15 g) were anesthetized with sodium pentobarbital (50 μg/g, i.p.), fluorescein sodium (12.5 μg/g) was i.v. injected. A segment of small intestine attached to its mesentery was loosely exteriorized for microscopic observation. Venules with diameters of 30 to 40 μm were selected to produce a microthrombus. In the epi-illumination system, the area of irradiation (wavelength above 520 nm) was approximately 50 μm in diameter on the focal plane. After the operation (15 min), the mouse was intravenously injected with PBS (control, 30 μl), aspirin, or kistomin through another lateral tail vein of the mouse. Five minutes after administration of these drugs, the irradiation by filtered light and the occlusion time was recorded.

Tail Bleeding Time. After anesthesia with sodium pentobarbital (50 μg/g, ip), male ICR mice (12–15 g) were intravenously injected with PBS (vehicle, 30 μl), aspirin, or kistomin through a lateral tail vein. After 5 min, the mouse was placed in a tube holder with its tail protruding, and then a cut 2 mm from the tail tip was made. The tail was immediately immersed vertically in normal saline at 37°C. Bleeding time was recorded from the time bleeding started until it completely stopped.

Results

Protein Sequencing and cDNA Cloning of Kistomin. To have an insight on kistomin's primary structure, protein sequencing was performed. A 14-kDa autoproteolytic fragment from kistomin was sequenced, and its N-terminal was revealed as LSKRKPHNDAQFLTNKDFDG (fragment 1). Moreover, two peptide sequences, VDKHNGNIKKIE (fragment 2) and APEVNNNPTKKFSDC (fragment 3), were obtained from CNBr digestion of kistomin.

To further determine the cDNA sequence of kistomin precursor, cDNA cloning was performed. Two primers in accordance with the conserved PKMCGV sequence of SVMP and the autoproteolytic fragment were used in the first amplification of kistomin cDNA. After screening of the *C. rhodostoma* cDNA library, a clone with approximately ~900 bp was obtained, representing the kistomin precursor presequence containing the partial metalloproteinase domain of kistomin (data not shown). To obtain the remaining cDNA sequence of kistomin, a pair of primers according to the sequences from kistomin-CNBr-digested fragment (VDKHNGNIKKIE) and vector was used. Figure 1 showed the assembled cDNA sequence and the deduced amino acid sequence of the kistomin precursor. Three partial sequences obtained from direct protein sequencing were found in the deduced amino acid sequence with 100% identity (Fig. 1, underlined sequences), indicting that it is a kistomin precursor. The precursor, designated prokistomin, consists of a presequence, prosequence, and a metalloproteinase domain and belongs to a P-I SVMP. A putative start site was indicated, and mature kistomin predicted from this site was 227 residues (Fig. 1), which was estimated to be 25.7 kDa. The deduced amino acid sequence of prokistomin contains the characteristic zinc-chelating sequence HEIGHNLGMEHD (Fig. 1, catalytic site), which is similar to that of other SVMPs, such as fibrolase (Randolph et al., 1992) and jararhagin (Paine et al., 1992).

Kistomin Inhibited Ristocetin-Induced Platelet Agglutination and Aggregation. To re-examine kistomin's activity in inhibiting platelet function, PS agglutination and PRP aggregation were performed. As shown in Fig. 2, kistomin concentration-dependently inhibited ristocetin-induced platelet agglutination and aggregation with a half-maximal inhibition concentration (IC_{50}) at 2.04 μg/ml (0.079 μM) and 8.25 μg/ml (0.321 μM), respectively. However, this inhibition was abolished by the treatment of kistomin with EDTA or *o*-phenanthrolene (data not shown), indicating the involvement of an enzymatic reaction.

Kistomin Cleaved Platelet GPIbα. To further elucidate the possible action mechanism of kistomin in inhibiting ristocetin-induced platelet aggregation, GPIbα expression on platelets was analyzed by flow cytometry and Western blotting. As depicted in immunofluorescence staining with anti-GPIbα mAb SZ2, kistomin treatment rapidly reduced the level of GPIbα expression on platelets, whereas the expression of the other two important platelet receptors, namely αIIbβ3 and α2β1 integrins, was not affected (Fig. 3A).

To characterize the proteolytic properties of kistomin on platelet GPIbα, Western blotting was performed. It was found that platelet intact GPIbα (~140 kDa) was cleaved by kistomin in a time-dependent manner, which could be abolished by EDTA (Fig. 3B). One intact GPIbα and two fragments migrated at molecular masses of ~140, ~130, and ~45 kDa, respectively, were detected by anti-GPIbα SZ2 mAb in total platelet lysate (arrows). We were surprised to find that only two fragments (~130 and ~45 kDa) were detected in supernatant (Fig. 3C), indicating that kistomin cleaves platelet GPIbα at two distinct sites to generate two soluble fragments, which can be recognized by the SZ2 mAb.

Binding of Kistomin to GPIbα. Because platelet GPIbα was cleaved by kistomin, we next investigated whether kistomin bound to GPIbα. To stop kistomin's enzymatic activity, the experiment was performed at 4°C. Under this condition, kistomin bound to GPIbα and replaced anti-GPIbα M45 mAb binding to platelets in a concentration-dependent manner (Fig. 4A). Binding of kistomin to GPIbα concentration-dependently increased and reached saturation at the concentrations more than 20 μg/ml (Fig. 4B). This result was confirmed by the observation that immobilized kistomin directly interacted with GPIbα in platelet lysate. It is noteworthy that this binding was not affected in the presence of EDTA (Fig. 4C), suggesting that bivalent cations are not required in this interaction. A similar binding ability was also found in immobilized agglucetin, a tetrameric GPIbα-binding protein from *A. acutus* (Wang and Huang, 2001), in which it migrated as two distinct bands at 16.2 and 14.5 kDa (Fig. 4, lane 3). In contrast, rhodostomin, an RGD-containing disintegrin purified from *C. rhodostoma* venom (Huang et al., 1987), failed to bind platelet GPIbα (data not shown).

Effect of Kistomin on the Multimeric Structure of vWF. We have shown that kistomin could bind and cleave platelet GPIbα (Fig. 3 and 4). To further examine whether kistomin affected multimeric structure of vWF, human vWF preincubated with or without kistomin was added to platelet suspension and ristocetin-induced platelet agglutination was

measured. Figure 5A showed that ristocetin-induced agglutination was time-dependently reduced under this condition but almost fully restored by re-adding a new intact vWF. Further analysis revealed that high-molecular-mass multimers of vWF obviously decreased and the low-molecular-mass multimers concomitantly increased in the presence of kistomin (Fig. 5B, lanes 1 and 2). Again, the cleavage of vWF by kistomin was abolished in the presence of EDTA or *o*-phenanthrolene (Fig. 5B, lanes 3 and 4). Taken together, our results indicate that kistomin can bind and cleave platelet GPIbα and vWF and subsequently inhibits vWF-induced platelet agglutination and aggregation.

Kistomin Affected Thrombosis and Hemostasis in Vivo. We next investigated whether kistomin exerted antithrombotic effect in vivo. It was shown that kistomin potently decreased antibody binding to platelet GPIbα in human whole blood, whereas crotalin and triflamp, two P-I SVMPs purified from venom of *C. atrox* (Wu et al., 2001b) and *T. flavoviridis* (Tseng et al., 2004a), respectively, were less effective at the same concentration in cleaving GPIbα (Fig. 6). We therefore hypothesized that kistomin could be an active protease in both in vitro and in vivo conditions. To confirm this hypothesis, we measured ex vivo platelet aggregation in PRP or PS prepared from kistomin-pretreated mouse. Be-

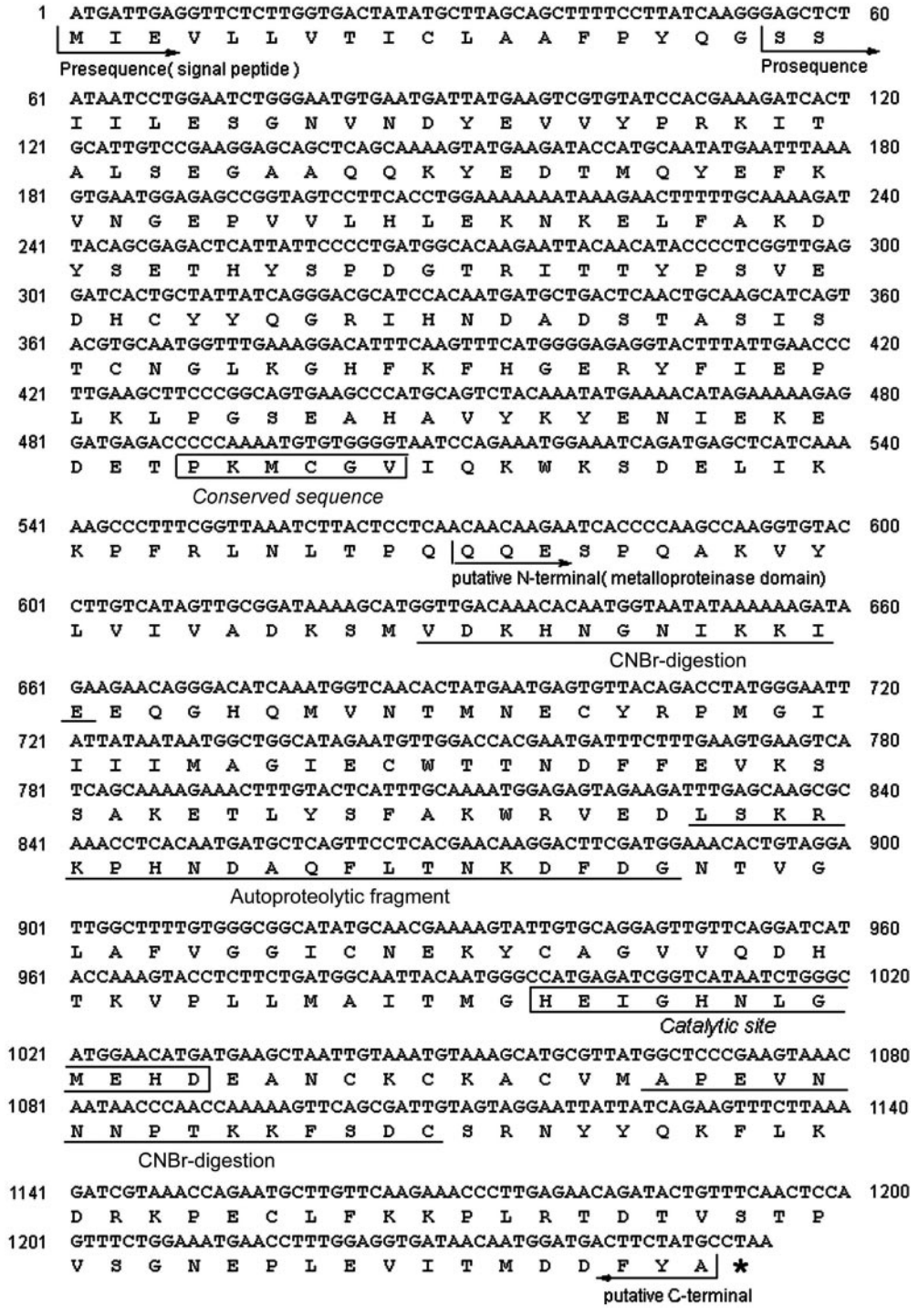

Fig. 1. cDNA sequence and deduced amino acid sequence of the putative protein precursor of kistomin. The sequence shown begins with the presequence, and the translation stop codon is indicated by an asterisk (*). Three fragments from CNBr-digested and autoproteolytic kistomin are indicated by underlines.

cause ristocetin is ineffective in causing platelet aggregation in mouse PRP, a snake venom-derived GPIbα agonist, gramicetin, was used in this assay (Wu et al., 2001a). As shown in Fig. 7A, gramicetin-induced platelet agglutination was inhibited by the GPIbα antagonist, agkistin, suggesting that a GPIbα-mediated pathway was involved in this agglutination. The agglutination was suppressed in PRP prepared from mouse treated with kistomin (Fig. 7B); however, collagen-, ADP-, convulxin- and thrombin-induced platelet aggregation was not significantly affected (Fig. 7, C–F). Thus, kistomin

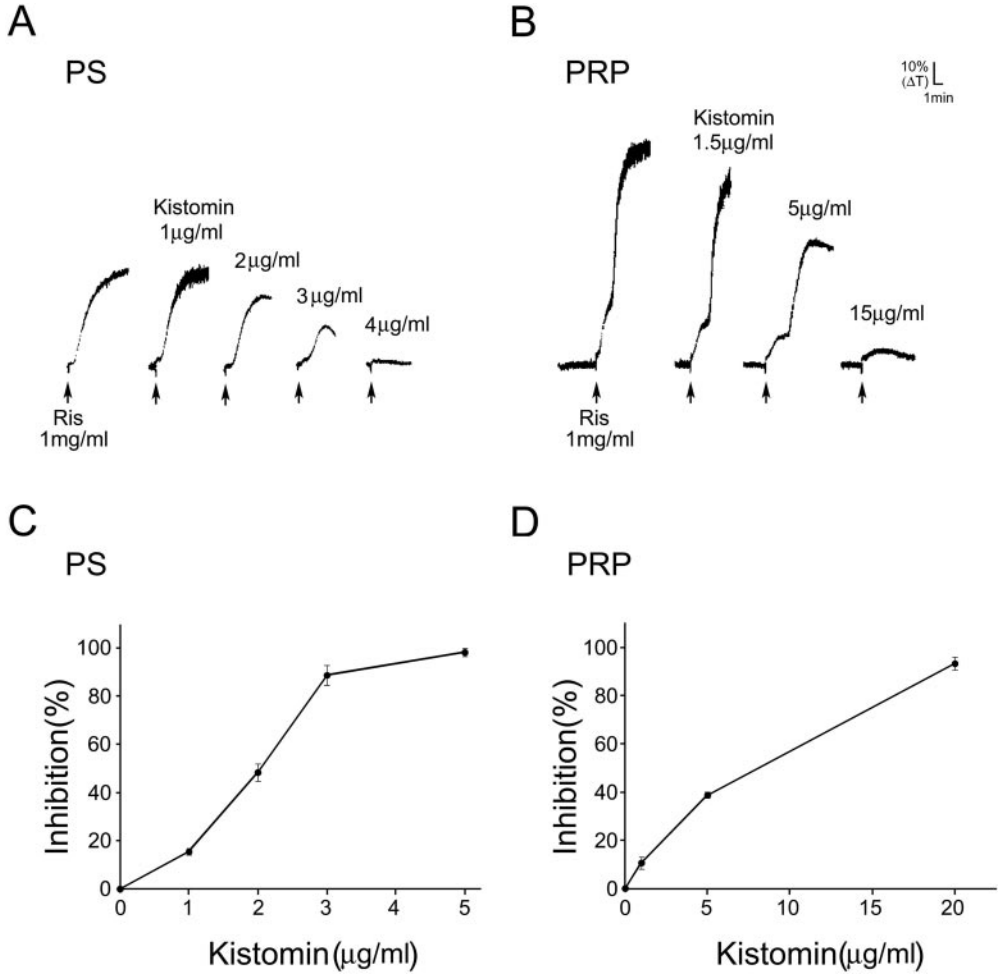

Fig. 2. Effect of kistomin on ristocetin-induced platelet agglutination and aggregation. Washed PS (A) and PRP (B) were pretreated with various concentrations of kistomin before the addition of ristocetin (1 mg/ml, arrow). Platelet agglutination and aggregation were monitored by turbidimetry in aggregometer. C and D, quantitative analysis of the data from A and B and similar experiments were performed. Data are presented as percentage of control and are mean ± S.E.M. ($n \geq 3$).

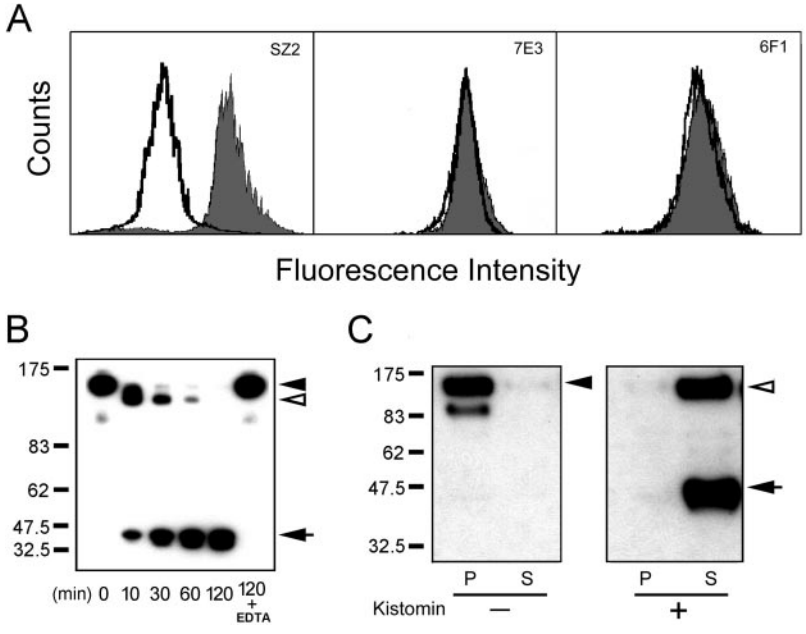

Fig. 3. Effect of kistomin on platelet GPIbα. A, flow cytometric analysis of GPIbα expression on platelets. Washed platelets treated with PBS (gray area) or kistomin (5 μg/ml, open area) at 37°C for 10 min were incubated with anti-GPIbα (SZ2), anti-αIIbβ3 (7E3) or anti-α2β1 (6F1) mAbs and subjected to be analyzed by flow cytometry. B and C, Western blot analysis of GPIbα expression on platelets. Washed platelets were treated with kistomin (20 μg/ml) at 37°C for (B) different duration as indicated or (C) for 30 min in the absence or presence of EDTA. Total cell lysates, cells pellets (P), and supernatant (S) were obtained as described under *Materials and Methods* and analyzed by Western blotting. An arrowhead indicates an intact GPIbα expression on platelet. Note that 130-kDa (open arrowheads) and 45-kDa fragments (arrows) were observed in total cell lysates (B) and in the supernatant (C) of kistomin-treated platelets. This experiment is representative of at least three similar experiments.

impaired mouse platelet function specifically through affecting GPIbα in vivo.

We then determined kistomin's antithrombotic effects in vivo. In fluorescent dye-treated mice, thrombus formation was observed in irradiated mesenteric venules of mice. The occlusion time of irradiated vessels was 134.3 $\pm$ 6.2 s in control mice (n = 12) but was prolonged to 173.2 $\pm$ 26.7 s (n = 13) and 301.9 $\pm$ 43.5 s (n = 10) by aspirin at doses of 150 and 250 μg/g, respectively. We were surprised to find that compared with aspirin, kistomin also exerted potent antithrombotic effect in vivo, prolonging the occlusion time to 194.9 $\pm$ 12.5 s (n = 10) and 273.2 $\pm$ 16.2 s (n = 10) at doses of 1.5 and 7 μg/g, respectively (Table 1). Kistomin was approximately 4000-fold more potent than aspirin in prolonging microvessel occlusion time on a molar basis. In parallel, the tail bleeding time of mice (control, 90.8 $\pm$ 5.0 s, n = 17) was prolonged to 172.1 $\pm$ 26.3 s and more than 1800 s by kistomin at the given doses of 1.5 and 7 μg/g, respectively. In contrast, aspirin at 150 and 250 μg/g also increased bleeding time to 559 $\pm$ 48.9 s (n = 13) and more than 1800 s (n = 10), respectively (Table 2).

Discussion

Platelet GPIbα-vWF interaction has been identified as an important target for therapeutics to prevent ischemic cardiovascular events (Jackson and Schoenwaelder, 2003). We have found that kistomin inhibited ristocetin-induced platelet agglutination in platelet suspension (Huang et al., 1993); however, its action mechanism, antithrombotic activity, and structure-activity relationship are still largely unknown. In this study, we demonstrated that kistomin is capable of binding to platelet GPIbα and cleaves GPIbα and vWF, exhibiting potent antiplatelet and antithrombotic activities in vitro and in vivo. More importantly, cDNA encoding kistomin precursor was cloned and revealed that mature kistomin is a P-I SVMP with only a metalloproteinase domain. The sequence of kistomin is shown with 51% identity to the P-I SVMP fibrolase, a fibrinolytic enzyme from *Agkistrodon contortrix contortrix* venom (Randolph et al., 1992), and with 40% identity to the P-III SVMP jararhagin, an $\alpha 2\beta 1$- and vWF-cleavage protease from *Bothrops jararaca* venom (Paine et al., 1992). Moreover, kistomin shares 29% identity with the proteinase domain of human ADAMTS13 (a disintegrin and metalloproteinase with thrombospondin motifs 13), an endogenous metalloproteinase specifically cleaving between

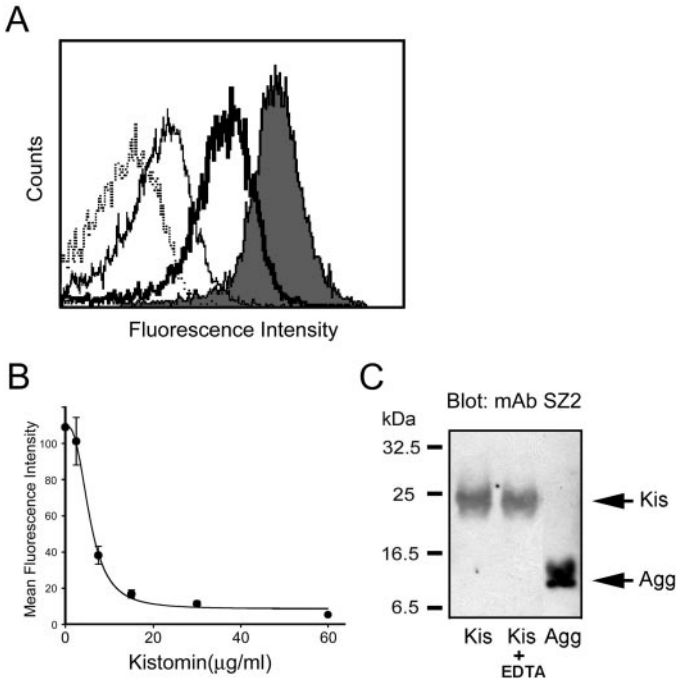

Fig. 4. Kistomin binds to platelet GP Ibα. A, kistomin competitively replaced anti-GPIbα mAb binding to platelets. Human washed platelets were incubated with PBS (gray area) or various concentrations of kistomin (open areas, 15, 30, and 60 μg/ml) at 4°C for 30 min, followed by incubation with FITC-conjugated anti-GPIbα mAb, M45, and then analyzed by flow cytometry. The histogram was representative from three similar experiments. B, quantitative analysis of binding assay data from A and similar experiments were performed. Data were expressed as mean fluorescence and were mean $\pm$ S.E. (n = 3) C, platelet GPIbα bound to immobilized kistomin. Kistomin (Kis, 20 μg) pretreated with vehicle or EDTA (10 mM) and agglucetin (agg, 15 μg) were applied to SDS-PAGE and transferred to PVDF membrane. The membrane was incubated with platelet total lysate and followed by Western blot analysis using anti-GPIbα mAb, SZ2. This experiment is a representative one of at least three similar experiments.

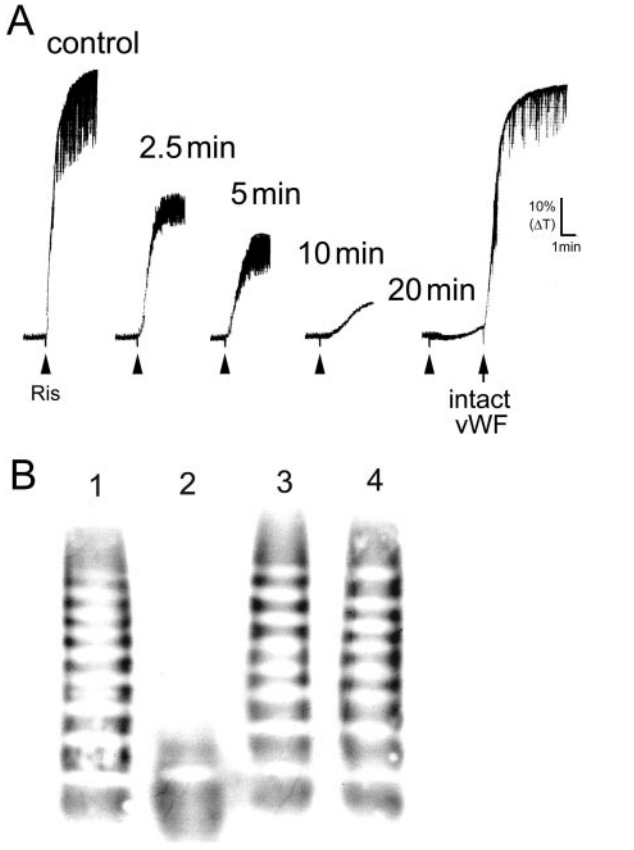

Fig. 5. Effect of kistomin on the multimeric structure of vWF. A, pretreatment of vWF with kistomin compromised vWF-induced platelet aggregation. Washed human platelets was incubated with kistomin (3 μg/ml)-pretreated vWF (10 μg/ml) at 37°C for the indicated times and ristocetin (ris, 1 mg/ml) was added to induce platelet aggregation. In the case of prior coincubation of vWF and kistomin for 20 min, intact vWF (10 μg/ml, arrow) was readded 3 min after addition of ristocetin. B, kistomin cleaved the mulitmeric structure of vWF. Human vWF (0.5 μg) was incubated at 37°C for 30 min with PBS (lane 1), kistomin (15 μg/ml, lane 2), EDTA (10 mM)-treated kistomin (lane 3), or *o*-phenanthrolene (10 mM)-treated kistomin (lane 4). Aliquots of each reaction mixture were subjected to SDS-1% agarose electrophoresis and vWF multimer were detected by peroxidase-conjugated anti-vWF antibody after blotting to a PVDF membrane. This experiment is representative of at least three similar experiments.

Tyr842 and Met843 in the A2 domain of vWF to regulate its physiological hemostatic activity (Levy et al., 2001). Being a P-I SVMP without an additional disintegrin/cysteine-rich domain, kistomin still has a relative strong selectivity toward platelet GPIbα and vWF, suggesting that the additional domain(s) is not necessarily required for the substrate recognition. From the protein chemistry and evolutionary viewpoint, it is an interesting issue to know why these SMVPs and matrix metalloproteniases have a similar specificity for GPIbα and/or vWF.

Kistomin inhibits vWF-induced platelet agglutination and aggregation through acting on platelet GPIbα and vWF. Several lines of evidence indicate that the platelet GPIbα and vWF were cleaved by kistomin during their coincubation. First, a significantly reduced binding signal in flow cytometry was observed after platelets were treated with kistomin (Fig. 3A). Second, the outer membrane portion of GPIbα was cleaved from platelet membrane into supernatant in the presence of kistomin and generated two soluble fragments, which migrated at the molecular masses of 45 and 130 kDa (Fig. 3, B and C). Third, kistomin competitively inhibited anti-GPIbα mAb interaction with platelet and directly bound to platelet GPIbα, as determined by flow cytometry and Western blotting (Fig. 4). Fourth, vWF-induced platelet agglutination was compromised by a preincubation of vWF with kistomin but reversed by adding an intact vWF (Fig. 5A). Fifth, upon kistomin incubation, high molecular mass multimers of vWF generated low molecular mass multimers (Fig. 5B). Last, EDTA pretreatment can abolish these activities of kistomin (Figs. 3, 5, and data not shown), indicating that kistomin is a typical SVMP, mediating antiplatelet activities through cleaving GPIbα and vWF.

Regarding specificity, the surface marker analysis showed that kistomin failed to affect the binding of anti-$\alpha 2\beta 1$ (6F1) and αIIbβ3 (7E3) mAbs to platelets. In contrast, kistomin specifically inhibited the binding of anti-GPIbα mAbs to platelets, including AP1, 6D1, and SZ2 (Fig. 3A and data not shown). Moreover, platelets prepared from kistomin-treated mice were unable to agglutinate in response to GPIbα-agonist induction but were able to aggregate in response to other agonists (Fig. 7), suggesting its relative specificity toward GPIbα both in vitro and in vivo. The GPIbα-binding epitopes for 6D1 and AP1 have been demonstrated to be located at the amino acid residues 104 to 128 and 201 to 268, respectively (Coller et al., 1983). SZ2 mAb has been shown to recognize anionic sulfated tyrosine residues 269 to 282 of GPIbα (Ward et al., 1996). Therefore, failed binding of these Abs to platelet in the presence of kistomin indicates that kistomin may cleave GPIbα, downstreaming the anionic tyrosine sulfated region. In Fig. 3, we found that outer membrane portion of GPIbα was cleaved by kistomin to generate a ~130-kDa soluble fragment. Because it was a soluble fragment found in total cell lysate and in the supernatant (Fig. 3C), the possibility of cleavage of GPIbα at the site near N terminus was excluded. Therefore, the first cleavage site was hypothesized to be located near C terminus of GP Ibα. The cytoplasmic tail of GPIbα contains 96 amino acid residues (Berndt et al., 2001) and is estimated to have a molecular mass of approximately 10 kDa. Therefore, the first cleavage site on GPIbα

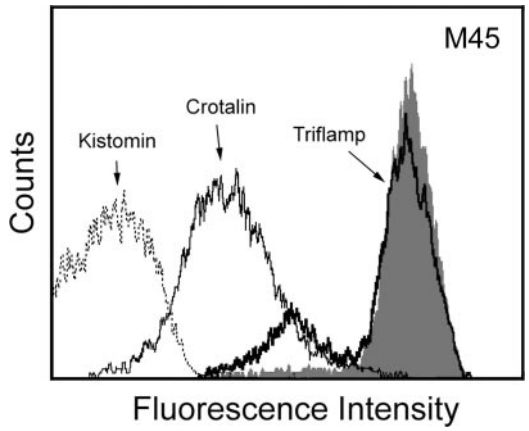

Fig. 6. Kistomin cleaves GPIbα in whole blood. Human whole blood was pretreated with PBS (gray area) and the indicated SVMPs (open areas, 100 μg/ml for each) at 37°C for 15 min. Samples were probed by FITC-conjugated anti-GPIbα M45 antibody and immediately analyzed by flow cytometry. This experiment is representative of at least three similar experiments.

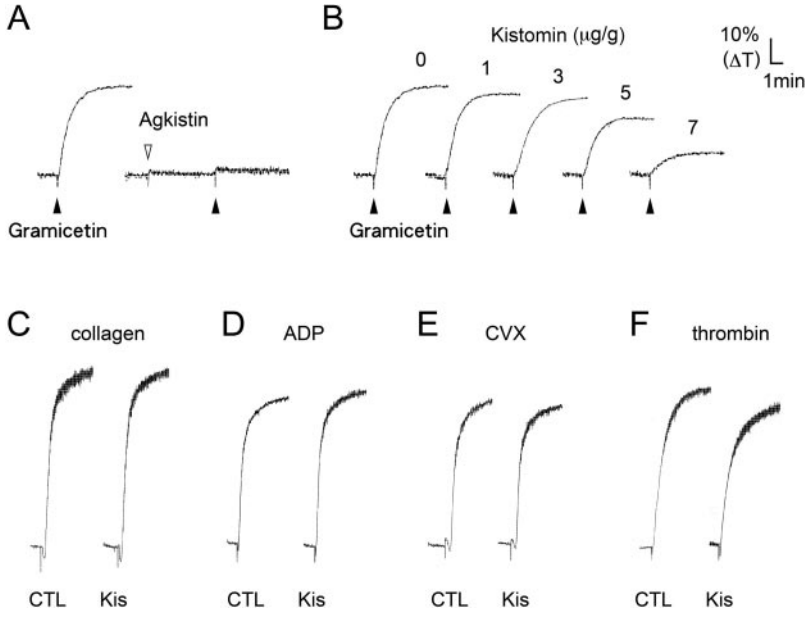

Fig. 7. Ex vivo test regarding the effects of kistomin on mouse platelets. A, GP Ibα antagonist inhibited gramicetin-induced platelet agglutination. Mouse PRP was treated with PBS or agkistin (5 μg/ml) and platelet agglutination was induced by adding gramicetin (1 μg/ml, solid arrow). B, PRP was prepared from mice treated with vehicle or the indicated doses of kistomin and gramicetin-induced platelet agglutination was measured by aggregometry. PRP (C–E) or PS (F) was prepared from mice treated with vehicle or kistomin (kis; 7 μg/g). Induction of platelet aggregation was done by adding collagen (10 μg/ml), ADP (20 μM), convulxin (cvx; 1.5 μg/ml), and thrombin (0.1 U) and was measured by aggregometry. This experiment is representative of at least three similar experiments.

may be located near the outer membrane of platelet. Second, a ~45-kDa soluble fragment increased gradually accompanying with a decrease of the ~130-kDa fragment (Fig. 3), suggesting that kistomin's second cleavage site is located within the ~130 kDa GPIbα fragment. This is evidenced by the observations that inactivated kistomin competitively replaced the binding of anti-GPIbα M45 mAb, which recognizes anionic sulfated tyrosine residues of GPIbα (Fig. 4). Kistomin seems to act like mocarhagin, a P-III SVMP, by cleaving GPIbα at a single site between Glu282 and Asp283 to generate a ~40-kDa fragment. However, this ~45-kDa fragment could be recognized by SZ2 on Western blotting analysis (Fig. 3, B and C), indicating that the binding epitope of SZ2, anionic sulfated tyrosine residues of GPIbα, still remained on the fragment. According to the size of the second fragment (~45kDa) and the binding epitopes of anti-GPIbα mAbs (SZ2 and M45), we postulated that the second kistomin-cleavage site on GPIbα is near downstream of the anionic sulfated tyrosine region. Taken together, we suggest that kistomin cleaves GPIbα at two distinct sites, one of which is located at the region near the outer membrane and another locates near anionic sulfated tyrosine. Kistomin's exact cleavage sites on GPIbα are still under investigation in our laboratory.

Our study also demonstrated that kistomin potently cleaved platelet GPIbα in human whole blood, compared with crotalin and triflamp, two P-I SVMPs (Fig. 6). It has been shown that human α2-macroglobulin and mouse macroglobulin are abundant in serum and capable of inhibiting and neutralizing the proteolytic activity of most proteinases, including some SVMPs (Tseng et al., 2004b). However, in this report, kistomin was demonstrated to elicit its antiplatelet and antithrombotic in vivo (Fig. 7 and Tables 1 and 2). These suggest that kistomin is less susceptible to be neutralized by globulins in serum and possibly can be developed as an antithrombotic agent. This is supported by the data shown in Tables 1 and 2, in which aspirin (150 μg/g) and kistomin both delayed the irradiation-induced occlusion time to a similar degree, but kistomin seems to be safer at a lower dose (1.5 μg/g) than aspirin in causing bleeding.

In conclusion, in this report we demonstrated that a P-I SVMP, kistomin, blocked vWF-induced platelet activation by specifically cleaving platelet GPIbα and vWF, suggesting that a metalloproteinase without an additional disintegrin/cysteine-rich domain has a relative specificity for GPIbα and vWF. More importantly, kistomin exerted an antithrombotic effect in vivo with certain properties quite different from those of P-I SVMPs derived from other snake venoms. Therefore, kistomin may be useful as a tool for studying the function of vWF-GPIbα, providing an alternative approach for the designing of antithrombotic agents.

TABLE 1

Effect of kistomin on fluorescent dye-induced platelet-rich thrombus formation in mesenteric venules of mice

Values are presented as means ± S.E.M. of experimental number (n) indicated

	Occlusion Time	n
	s	
Control (PBS)	134.3 ± 6.2	12
Aspirin		
150 μg/g	172.6 ± 6.3***	16
250 μg/g	287.4 ± 15.2***	13
Kistomin		
1.5 μg/g	194.9 ± 12.5***	10
7 μg/g	273.2 ± 16.2***	10

*** $P < 0.001$ compared with control.

TABLE 2

Effect of kistomin on the tail bleeding time of mice

Values are presented as means ± S.E.M. of experimental number (n) indicated.

	Tail Bleeding Time	n
	s	
Control (PBS)	90.8 ± 5.1	17
Aspirin		
150 μg/g	559.0 ± 48.9***	15
250 μg/g	>1800.0***	15
Kistomin		
1.5 μg/g	172.1 ± 26.3**	17
7 μg/g	>1800.0***	13

** $P < 0.01$ compared with control.
*** $P < 0.001$ compared with control.

Acknowledgments

We appreciate the generous supply of mAbs from Dr. B. S. Coller (7E3, 6D1, and 6F1) and Dr. R. R. Montgomery (AP1). We also thank Dr. L.P. Chow for protein sequencing.

References

Andrews RK and Berndt MC (2004) Platelet physiology and thrombosis. *Thromb Res* **114:**447–453.

Andrews RK, Gardiner EE, Shen Y, Whisstock JC, and Berndt MC (2003) Glycoprotein Ib-IX-V. *Int J Biochem Cell Biol* **35:**1170–1174.

Berndt MC, Shen Y, Dopheide SM, Gardiner EE, and Andrews RK (2001) The vascular biology of the glycoprotein Ib-IX-V complex. *Thromb Haemost* **86:**178–188.

Bonnefoy A, Vermylen J, and Hoylaerts MF (2003) Inhibition of von Willebrand factor-GPIb/IX/V interactions as a strategy to prevent arterial thrombosis. *Expert Rev Cardiovasc Ther* **1:**257–269.

Canobbio I, Balduini C, and Torti M (2004) Signalling through the platelet glycoprotein Ib-V-IX complex. *Cell Signal* **16:**1329–1344.

Chang MC and Huang TF (1994) In vivo effect of a thrombin-like enzyme on platelet plug formation induced in mesenteric microvessels of mice. *Thromb Res* **73:**31–38.

Coller BS, Peerschke EI, Scudder LE, and Sullivan CA (1983) Studies with a murine monoclonal antibody that abolishes ristocetin-induced binding of von Willebrand factor to platelets: additional evidence in support of GPIb as a platelet receptor for von Willebrand factor. *Blood* **61:**99–110.

Fox JW and Serrano SMT (2005) Structural considerations of the snake venom metalloproteinases, key members of the M12 reprolysin family of metalloproteinases. *Toxicon* **45:**969–985.

Huang TF, Chang MC, and Teng CM (1993) Antiplatelet protease, kistomin, selectively cleaves human platelet glycoprotein Ib. *Biochim Biophys Acta* **1158:**293–299.

Huang TF, Wu WJ, and Ouyang C (1987) Characterization of a potent platelet aggregation inhibitor for *Agkistrodon rhodostoma* snake venom. *Biochim Biophys Acta* **925:**248–257.

Jackson SP and Schoenwaelder SM (2003) Antiplatelet therapy: in search of the 'magic bullet'. *Nat Rev Drug Discov* **2:**775–789.

Kamiguti AS (2005) Platelets as targets of snake venom metalloproteinases. *Toxicon* **45:**1041–1049.

Levy GG, Nichols WC, Lian EC, Foroud T, McClintick JN, McGee BM, Yang AY, Siemieniak DR, Stark KR, Gruppo R, et al. (2001) Mutations in a member of the ADAMTS gene family cause thrombotic thrombocytopenic purpura. *Nature* 413: 488–494.

Liu CZ, Hur BT, and Huang TF (1996) Measurement of glycoprotein IIb/IIIa blockade by flow cytometry with fluorescein isothiocyanate-conjugated crotavirin, a member of disintegrins. *Thromb Haemost* **76:**585–591.

Marsh NA (2001) Diagnostic uses of snake venom. *Haemostasis* **31:**211–217.

Matsui T, Fujimura Y, and Titani K (2000) Snake venom proteases affecting hemostasis and thrombosis. *Biochim Biophys Acta* **1477:**146–156.

Paine MJ, Desmond HP, Theakston RD, and Crampton JM (1992) Purification, cloning, and molecular characterization of a high molecular weight hemorrhagic metalloprotease, jararhagin, from *Bothrops jararaca* venom. Insights into the disintegrin gene family. *J Biol Chem* **267:**22869–22876.

Randolph A, Chamberlain SH, Chu HLC, Retzios AD, Markland FS Jr and Masiarz FR (1992) Amino acid sequence of fibrolase, a direct-acting fibrinolytic enzyme from *Agkistrodon contortrix contortrix* venom. *Protein Sci* **1:**590–600.

Tseng YL, Lee CJ, and Huang TF (2004a) Effects of a snake venom metalloproteinase, triflamp, on platelet aggregation, platelet-neutrophil and neutrophil-neutrophil interactions: involvement of platelet GPIbalpha and neutrophil PSGL-1. *Thromb Haemost* **91:**315–324.

Tseng YL, Wu WB, Hsu CC, Peng HC, and Huang TF (2004b) Inhibitory effects of human alpha2-macroglobulin and mouse serum on the PSGL-1 and glycoprotein Ib proteolysis by a snake venom metalloproteinase, triflamp. *Toxicon* **43:**769–777.

Wang WJ and Huang TF (2001) A novel tetrameric venom protein, agglucetin from *Agkistrodon acutus*, acts as a glycoprotein Ib agonist. *Thromb Haemost* **86:**1077–1086.

Ward CM, Andrews RK, Smith AI, and Berndt MC (1996) Mocarhagin, a novel cobra venom metalloproteinase, cleaves the platelet von Willebrand factor receptor glycoprotein Ibalpha. Identification of the sulfated tyrosine/anionic sequence Tyr-276-Glu-282 of glycoprotein Ibalpha as a binding site for von Willebrand factor and alpha-thrombin. *Biochemistry* **35:**4929–4938.

Wu WB, Chang SC, Liau MY, and Huang TF (2001a) Purification, molecular cloning and mechanism of action of graminelysin I, a snake-venom-derived metalloproteinase that induces apoptosis of human endothelial cells. *Biochem J* **357:**719–728.

Wu WB, Peng HC, and Huang TF (2001b) Crotalin, a vWF and GPIb cleaving metalloproteinase from venom of *Crotalus atrox*. *Thromb Haemost* **86:**1501–1511.

Address correspondence to: Tur-Fu Huang, Department of Pharmacology, College of Medicine, National Taiwan University, No1, Sec1, Jen-Ai Rd, Taipei, Taiwan. E-mail: turfu@ntu.edu.tw